

## Manipulating the Production and Recombination of Electrons during Electron Transfer: Femtosecond Control of the Charge-Transfer-to-Solvent (CTTS) Dynamics of the Sodium Anion

Ignacio B. Martini, Erik R. Barthel, and Benjamin J. Schwartz\*

*Contribution from the Department of Chemistry and Biochemistry, University of California, Los Angeles, California 90095-1569*

Received February 14, 2002

**Abstract:** The scavenging of a solvated electron represents the simplest possible electron-transfer (ET) reaction. In this work, we show how a sequence of femtosecond laser pulses can be used to manipulate an ET reaction that has only electronic degrees of freedom: the scavenging of a solvated electron by a single atom in solution. Solvated electrons in tetrahydrofuran are created via photodetachment using the charge-transfer-to-solvent (CTTS) transition of sodide ( $\text{Na}^-$ ). The CTTS process ejects electrons to well-defined distances, leading to three possible initial geometries for the back ET reaction between the solvated electrons and their geminate sodium atom partners ( $\text{Na}^0$ ). Electrons that are ejected within the same solvent cavity as the sodium atom (immediate contact pairs) undergo back ET in  $\sim 1$  ps. Electrons ejected one solvent shell away from the  $\text{Na}^0$  (solvent-separated contact pairs) take hundreds of picoseconds to undergo back ET. Electrons ejected more than one solvent shell from the sodium atom (free solvated electrons) do not recombine on subnanosecond time scales. We manipulate the back ET reaction for each of these geometries by applying a "re-excitation" pulse to promote the localized solvated electron ground state into a highly delocalized excited-state wave function in the fluid's conduction band. We find that re-excitation of electrons in immediate contact pairs suppresses the back ET reaction. The kinetics at different probe wavelengths and in different solvents suggest that the recombination is suppressed because the excited electrons can relocalize into different solvent cavities upon relaxation to the ground state. Roughly one-third of the re-excited electrons do not collapse back into their original solvent cavities, and of these, the majority relocalize into a cavity one solvent shell away. In contrast to the behavior of the immediate pair electrons, re-excitation of electrons in solvent-separated contact pairs leads to an early time enhancement of the back ET reaction, followed by a longer-time recombination suppression. The recombination enhancement results from the improved overlap between the electron and the  $\text{Na}^0$  one solvent shell away due to the delocalization of the wave function upon re-excitation. Once the excited state decays, however, the enhanced back ET is shut off, and some of the re-excited electrons relocalize even farther from their geminate partners, leading to a long-time suppression of the recombination; the rates for recombination enhancement and relocalization are comparable. Enhanced recombination is still observed even when the re-excitation pulse is applied hundreds of picoseconds after the initial CTTS photodetachment, verifying that solvent-separated contact pairs are long-lived, metastable entities. Taken together, all these results, combined with the simplicity and convenient spectroscopy of the sodide CTTS system, allow for an unprecedented degree of control that is a significant step toward building a full molecular-level picture of condensed-phase ET reactions.

### I. Introduction

Solvated electrons ( $e^-_s$ ) are arguably the simplest chemical species that can exist in solution and serve as fundamental species in radiation chemistry,<sup>1</sup> biology,<sup>2</sup> and physics.<sup>3</sup> These

excess charges in a liquid reside in solvent cavities formed by the displacement of solvent molecules. Thus, the best zeroth-order picture for the electronic structure of a solvated electron is that of a particle in a finite, quasi-spherical box. For example, in polar fluids such as water, ammonia, or methanol, the potential well created by the solvent surrounding the excess electron is deep enough to support a bound s-like ground state as well as three quasi-degenerate bound p-like excited states,<sup>4</sup>

\* Corresponding author. Voice: (310) 206-4113. Fax: (310) 206-4038. E-mail: schwartz@chem.ucla.edu.

- (1) Warman, J. M. In *The Study of Fast Processes and Transient Species by Electron Pulse Radiolysis*; Baxendale, J. H., Bus, F., Eds.; Reidel: Dordrecht, 1983.
- (2) Pottinger, S. M. *Radiation Biology: a Textbook: General Consideration of Radiation Damage*; Mount Saint Scholastica College, Tape Institute: Atchinson, KS, 1962.
- (3) Dyson, N. A. *Radiation Physics with Applications in Medicine and Biology*; Horwood: New York, 1983.

- (4) See, e.g.: Rossky, P. J.; Schnitker, J. *J. Phys. Chem.* **1988**, *92*, 4277. Sprik, M.; Impey, R. W.; Klein, M. L. *J. Stat. Phys.* **1986**, *43*, 967. Romeo, C.; Jonah, C. D. *J. Chem. Phys.* **1989**, *90*, 1877. Barnett, R. B.; Landman, U.; Nitzan, A. *J. Chem. Phys.* **1989**, *90*, 4413. Turi, L.; Mosyak, A.; Rossky, P. J. *J. Chem. Phys.* **1997**, *107*, 1970.

resulting in an intense absorption band in the visible/near-IR.<sup>5</sup> In nonpolar fluids such as alkanes or ethers, however, the solvent cavity typically can support only the s-like ground electronic state,<sup>6</sup> leading to an absorption spectrum in the infrared that usually peaks near  $2 \mu\text{m}$ .<sup>7,8</sup> In both polar and nonpolar liquids, solvated electrons with sufficient energy can access unbound (delocalized) higher excited states lying in the conduction band of the fluid.

The nature of the surrounding solvent cavity controls not only the electronic structure but also the reactivity of the  $e^-_s$ . In water, for example, hydrated electrons are the simplest free radicals and therefore act as very strong reducing agents for most chemical species. The reactivity of the ground-state hydrated electron, however, is limited by the thermal fluctuations of the solvent cavity that allow the electron to come into contact with scavengers in solution. Thus, the reaction rate for electron scavenging reactions is limited by the diffusion of the reacting species into the same solvent cavity.<sup>9</sup> Once diffusion has done its work, it is the closest solvent molecules that determine how the charge of the solvated electron is transferred to the scavenger. Clearly, any detailed study of solvated electron reaction dynamics, which can be thought of as the simplest example of electron transfer (ET), needs to focus on the molecular details of the solvent motions surrounding the  $e^-_s$ .<sup>10</sup>

Recently, Barbara and co-workers used a sequence of three ultrafast laser pulses to measure the scavenging yields of different electronic states of the hydrated electron.<sup>11</sup> In these experiments, the first pulse created hydrated electrons via multiphoton ionization of water, the second pulse interrupted the diffusion-controlled back ET reaction by placing the hydrated electron into one of its electronic excited states, and then the third pulse was used to monitor how the second pulse altered the back ET reaction. After a careful analysis, these workers concluded that the rate of ET is proportional to the average electron density in contact with the scavenger.<sup>11</sup> For example, the p-like excited state of the hydrated electron has a volume  $\sim 5$  times larger than that of the ground state and therefore reacts  $\sim 5$  times slower, as long as the scavenger lies within the envelope of the electron's wave function. This makes sense from a Golden Rule perspective: the rate of nonadiabatic electron transfer should be determined by a matrix element that is proportional to the donor/acceptor orbital overlap.<sup>11</sup> While the use of the three-pulse sequence allowed Barbara and co-workers to obtain detailed information on the macroscopic reaction rate for the different electronic states of the  $e^-_s$ , these authors were unable to address the microscopic details of the

solvent motions driving ET due to the diffusive character of these reactions.

In this paper, we present a related series of experiments designed to elucidate the molecular details of the solvent motions that control the ET reactions of solvated electrons. The system we chose to study is the charge-transfer-to-solvent (CTTS)<sup>12</sup> reaction and subsequent back ET reaction of the sodium anion ( $\text{Na}^-$ , or sodide) in solution.<sup>13,14</sup> Theoretical calculations have shown that, in CTTS reactions, the Franck–Condon excitation produces a localized electronic state that is bound only by the polarization of the solvent around the solute.<sup>15</sup> It is this bound-to-quasi-bound transition that results in the intense CTTS absorption band exhibited by many anions.<sup>12</sup> Once this quasi-bound state is excited, the subsequent response to the excitation leads to a rearrangement of the solvent molecules that causes the electron to detach and localize into a nearby solvent cavity.<sup>16</sup> We have extensively studied the electron-transfer dynamics of sodide in previous work and determined that CTTS electron detachment produces molecularly well-defined sodium atom ( $\text{Na}^0$ ):solvated electron contact pairs.<sup>17–19</sup> Depending on the energy of the photon used to initiate CTTS detachment, we found that the ejected electron can reside either in the same solvent cavity as the Na atom (an “immediate contact pair”, which undergoes back ET in  $\sim 1$  ps), in an adjacent cavity separated by one solvent molecule from the Na atom (a “solvent-separated contact pair”, which takes hundreds of picoseconds to recombine), or in a solvent cavity far from the Na atom (a “free electron”, which does not recombine for at least 1 ns),<sup>19</sup> as depicted in Figure 1A.<sup>20</sup> Thus, the  $\text{Na}^-$  CTTS reaction provides the advantage that the back ET reaction is not diffusion controlled but instead proceeds between a well-defined contact-pair donor state and a well-defined sodium anion acceptor state. Moreover, the fact that this model system has only electronic degrees of freedom (i.e., it consists of only single atoms and electrons) means that any spectral changes that occur as the reaction proceeds must result from motions of the solvent molecules surrounding the reactants. In combination, these two advantages will allow us to unravel many of the molecular details underlying charge transfer by manipulating the  $e^-_s$  during the course of the ET reaction.

This paper follows up a preliminary report describing a series of three-pulse ultrafast experiments that we designed to manipulate the CTTS reaction of sodide in tetrahydrofuran (THF).<sup>21</sup>

- (5) See, e.g.: Hart, E. J.; Boag, J. W. *J. Am. Chem. Soc.* **1962**, *84*, 4090. Jou, F.-Y.; Freeman, G. R. *J. Phys. Chem.* **1979**, *83*, 2383.  
 (6) See, e.g.: Liu, Z.; Berne, B. J. *J. Chem. Phys.* **1993**, *99*, 9054.  
 (7) For a review, see: Davis, H. T.; Brown, R. G. *Adv. Chem. Phys.* **1975**, *31*, 329.  
 (8) Dorfman, L. M.; Jou, F. Y.; Wageman, R. *Ber. Bunsen-Ges. Phys. Chem.* **1971**, *75*, 681. Jou, F. Y.; Freeman, G. R. *Can. J. Phys.* **1976**, *54*, 3693.  
 (9) See, e.g.: Pimblott, S. M.; LaVerne, J. A. *J. Phys. Chem. A* **1998**, *102*, 2967.  
 (10) Most theoretical descriptions of ET reactions are based on Marcus theory, which assumes that the free energy surfaces for the reaction are parabolic in a solvent polarization coordinate. However, Marcus theory does not specify which solvent motions constitute the reaction coordinate. One of our goals from this work is to start building a molecular-level picture of how the solvent controls the dynamics of electron-transfer reactions; see ref 19.  
 (11) Son, D. H.; Kambhampati, P.; Kee, T. W.; Barbara, P. F. *J. Phys. Chem. A* **2001**, *105*, 8269. Kee, T. W.; Son, D. H.; Kambhampati, P.; Barbara, P. F. *J. Phys. Chem. A* **2001**, *105*, 8434. Son, D. H.; Kambhampati, P.; Kee, T. W.; Barbara, P. F. *Chem. Phys. Lett.* **2001**, *342*, 571.

- (12) Blandamer, M. J.; Fox, M. F. *Chem. Rev.* **1970**, *70*, 59.  
 (13) See, e.g.: Jortner, J.; Ottolenghi, M.; Stein, G. *J. Phys. Chem.* **1964**, *68*, 247. Lok, M. T.; Tehan, F. J.; Dye, J. L. *J. Phys. Chem.* **1972**, *76*, 2975.  
 (14) Early flash photolysis work on alkali metal anions can be found in the following: Huppert, D.; Rentzepis, P. M.; Struve, W. S. *J. Phys. Chem.* **1975**, *79*, 2850. Huppert, D.; Rentzepis, P. M. *J. Phys. Chem.* **1976**, *64*, 191.  
 (15) Sheu, W.-S.; Rossky, P. J. *J. Am. Chem. Soc.* **1993**, *115*, 7729. Chen, H. Y.; Sheu, W.-S. *J. Am. Chem. Soc.* **2000**, *122*, 7534. Combariza, J. E.; Kestner, N. R.; Jortner, J. *J. Chem. Phys.* **1994**, *101*, 2851. Bradforth, S. E.; Jungwirth, P. *J. Phys. Chem. A* **2002**, *106*, 1286.  
 (16) See, e.g.: Sheu, W.-S.; Rossky, P. J. *J. Chem. Phys. Lett.* **1993**, *213*, 233. Sheu, W.-S.; Rossky, P. J. *J. Phys. Chem.* **1996**, *100*, 1295. Staib, A.; Borgis, D. *J. Chem. Phys.* **1996**, *104*, 9027. Staib, A.; Borgis, D. *J. Chem. Phys.* **1996**, *104*, 4776.  
 (17) Barthel, E. R.; Martini, I. B.; Schwartz, B. J. *J. Chem. Phys.* **2000**, *112*, 9433.  
 (18) Martini, I. B.; Barthel, E. R.; Schwartz, B. J. *J. Chem. Phys.* **2000**, *113*, 11245.  
 (19) Barthel, E. R.; Martini, I. B.; Schwartz, B. J. *J. Phys. Chem. B* **2001**, *105*, 12230.  
 (20) This picture is also consistent with the photon energy dependence of the ejection yield for electrons from  $\text{Rb}^-$  in solution; see: Rozenstein, V.; Heimlich, Y.; Levanon, H.; Lukin, L. *J. Phys. Chem. A* **2001**, *105*, 3701.  
 (21) Martini, I. B.; Barthel, E. R.; Schwartz, B. J. *Science* **2001**, *293*, 462.

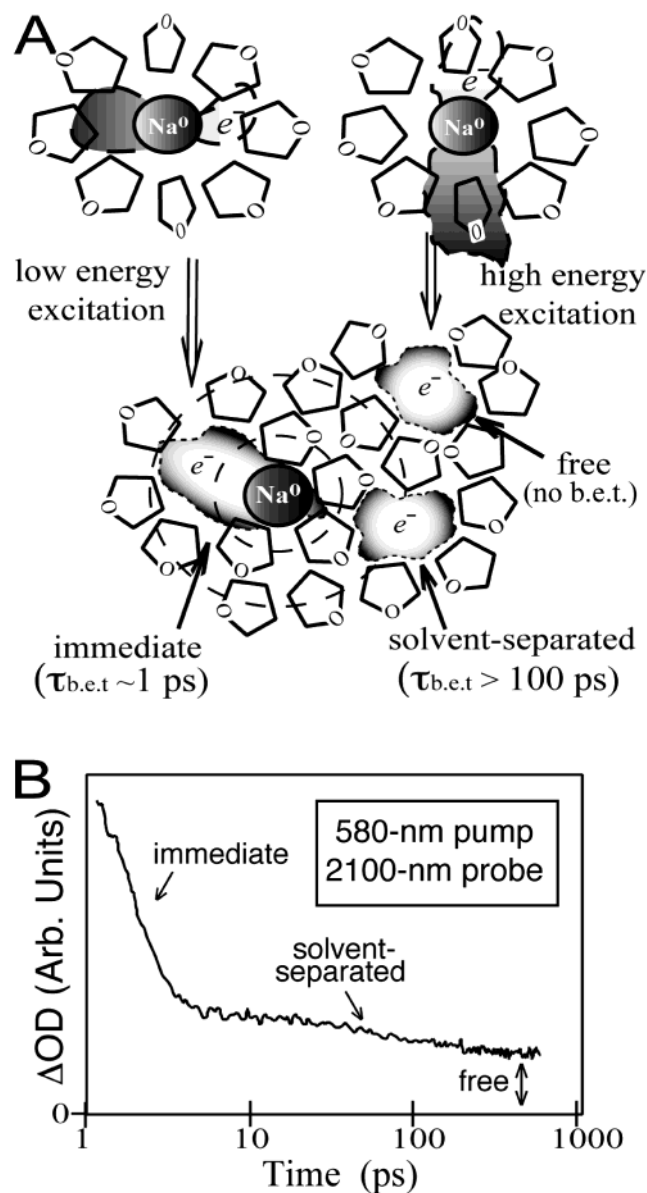


**Figure 1.** (A) Schematic representation of the important processes in the  $\text{Na}^+$  charge-transfer-to-solvent reaction. Low-energy CTTS excitation produces a p-like excited state that is primarily contained inside the original solvent cavity (upper left diagram). Solvent translational motions then lead to detachment of the electron into an immediate contact pair that recombines in  $\sim 1$  ps (left side of lower diagram). CTTS excitation with higher energy generates a spatially extended p-like wave function that extends beyond the original solvent cavity (upper right diagram). Depending on the degree of delocalization, the electron can then detach either into a metastable solvent-separated contact pair (lower right side of lower diagram), which recombines in hundreds of picoseconds, or a free solvated electron (upper right side of lower diagram), which does not recombine on subnanosecond time scales. (B) Typical sodide two-pulse pump–probe experiment on a logarithmic time scale. The 2100-nm probe pulse monitors the concentration of solvated electrons created by the 580-nm pump pulse. The signal decays on two distinctive time scales: the fast ( $\sim 1$  ps), large-amplitude component reflects the recombination of electrons in immediate contact pairs, while the smaller amplitude long ( $\sim 200$  ps) decay results from the recombination of solvent-separated contact pairs. The offset of the signal at long times is due to free solvated electrons that have not recombined.

In this preliminary work, we used the first pulse to excite the sodide CTTS band and produce solvated electron:sodium atom contact pairs. The second pulse was then used to re-excite the newly detached solvated electrons into a highly delocalized state in the fluid's conduction band. The fact that immediate contact

pairs undergo back ET much faster than solvent-separated pairs allowed us to selectively excite the  $e^-_s$  in either the immediate or solvent-separated pairs by applying the second pulse at early times or later times, respectively. The third pulse was then used to monitor the amount of  $\text{Na}^-$  produced by the back ET reaction following application of the first two pulses. We found that the second pulse suppressed the recombination of the immediate contact pairs, but that the recombination was both enhanced at short times and suppressed at longer times when the second pulse was applied to solvent-separated pairs. These results were explained by the idea that the second pulse acts to *relocalize* solvated electrons in THF: after an excited  $e^-_s$  relaxes from the conduction band, it resides in a cavity that can be some distance away from its original location before excitation.<sup>21</sup> It is this ability to relocate the electron during the course of the recombination that will allow us to start unraveling the details of the solvent motions underlying electron-transfer reactions.

In the rest of this paper, we examine in detail how controlling electron relocalization in the sodide system provides new insights into the molecular nature of ET. Section II describes the details of our experimental setup. For readers unfamiliar with our previous work, section III briefly reviews the spectroscopy and dynamics of the sodide CTTS reaction and explains our choice of this system by comparison to related work done on other systems. Section IV-A discusses how re-excitation suppresses the back ET reaction of immediate contact pairs by relocalization of the electrons into solvent-separated contact pairs, which recombine more slowly than the immediate pairs. In particular, we find that roughly one-third of the re-excited electrons relocalize, and that the majority of these do so into an adjacent solvent cavity rather than into the bulk of the solvent. We also argue that the relocalization of re-excited electrons is the same process as internal conversion: it is the collapse of the delocalized excited wave function back into a solvent cavity that causes relocalization. Section IV-B explores how re-excitation of the electrons in solvent-separated contact pairs leads to both accelerated recombination at early times and hindered recombination at longer times. Here we observe that roughly half of the solvent-separated electrons can undergo enhanced recombination upon re-excitation, the result of better overlap of the delocalized excited-state wave function with the sodium atom one solvent shell away. We also show that recombination enhancement can still take place at re-excitation times greater than 0.5 ns, verifying that solvent-separated contact pairs are metastable entities that live for hundreds of picoseconds. We conclude in section V by presenting a molecular-level picture that is consistent with all the results. In particular, the fact that relocalization occurs on a time scale similar to that of the original CTTS photodetachment suggests that similar solvent motions are responsible for the dynamics of all aspects of this model electron-transfer system.

## II. Experimental Setup

The laser system used for our three-pulse experiments has been described previously.<sup>22</sup> Briefly, a regeneratively amplified Ti:sapphire laser (Spectra Physics) produces  $\sim 1$ -mJ pulses at 780 nm of  $\sim 120$ -fs duration at a 1-kHz repetition rate. For the initial CTTS excitation to create  $e^-_s$  (pulse 1 in Figure 2, which we will refer to as the “pump”

(22) Nguyen, T.-Q.; Martini, I. B.; Liu, J.; Schwartz, B. J. *J. Phys. Chem. B* **2000**, *104*, 237.

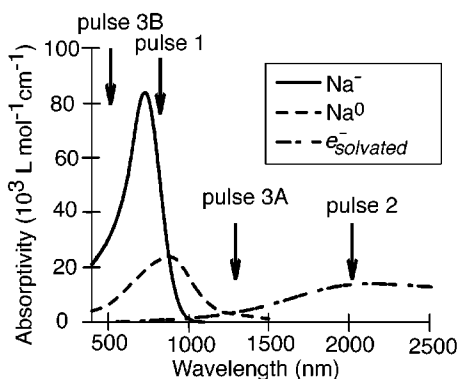


**Figure 2.** Steady-state absorption spectra of the important species involved in the CTTS reaction of sodide in THF: ground-state  $\text{Na}^-$  [solid curve]; the solvated neutral sodium atom [dashed curve; ref 32]; and the solvated electron [dot-dashed curve; ref 8]. The arrows show the spectral positions of the femtosecond laser pulses used in the experiments. Pulse 1 (pump) initiates the CTTS reaction; pulse 2 (re-excitation) changes the wave function of the newly detached solvated electron; and pulse 3 (probe) monitors the reaction dynamics of either the solvated electron (pulse 3A) or the newly recombined sodium anions (pulse 3B).

pulse), we used a surface reflection from the main beam, or in some cases its second harmonic at 390 nm generated in a BBO crystal. The remaining fundamental light was used to pump an optical parametric amplifier (OPA) that generates tunable signal and idler beams in the infrared. The “probe” pulse was generated by tuning the OPA signal beam to 1250 nm, where it either was used directly to probe the solvated electron’s absorption (pulse 3A in Figure 2) or was sum-frequency mixed with the residual 780-nm light to produce 480-nm pulses that probed the bleach recovery of  $\text{Na}^-$  (pulse 3B in Figure 2).<sup>23</sup> The OPA idler beam at  $\sim 2075$  nm was used to excite the photogenerated solvated electrons (pulse 2 in Figure 2, the “re-excitation” pulse).<sup>24</sup> The optical paths of both the pump and re-excitation pulses had a fixed length, while the probe pulse was retroreflected on a motorized translation stage that provided a computer-controlled variable delay. The relative arrival times of the pump and re-excitation pulses at the sample were controlled by inserting transparent optical materials (such as cover slips or optical filters) of known thickness into the beam path to achieve the desired optical delay. In some of the experiments using 390-nm pump pulses, however, the re-excitation pulse was routed through a set of mirrors that added at least 150 mm ( $\sim 500$  ps) delay relative to the pump pulse. All three beams were collinearly aligned and loosely focused into the 1-mm-path-length quartz cell containing the sample. The probe pulse was split into signal and reference beams that were detected with matched InGaAs (for 1250-nm probe experiments) or Si (for 480-nm probe experiments) photodiodes. The outputs of the photodiodes were digitized on a shot-by-shot basis using a fast gated current-integrating analog-to-digital converter.<sup>22</sup> For the three-pulse experiments presented in this paper, sensitivities better than 0.1 mOD are achieved with this experimental setup after signal averaging for  $\sim 60$  min.

In our typical two-pulse pump–probe experiment, a mechanical chopper is placed in the pump beam, and the differential transmission of the probe beam is determined at each position of the translation stage. The differential transmission was measured by subtracting the counts measured on the reference diode from those measured on the

signal diode and then dividing this difference by the number of counts on the reference diode. This procedure was done on a shot-by-shot basis, and the results were accumulated for shots when the pump was both blocked and unblocked. To avoid deleterious effects from laser intensity fluctuations, shots for which the pulse intensities fell outside a preset range were rejected. After 600 acceptable shots were collected (300 each with the pump blocked and unblocked), the averaged differential transmission data with the pump unblocked were normalized against the averaged data with the pump blocked, the translation stage was moved to the next position, and then the entire process was repeated. Computed in this way, transient bleaching signals show a positive differential transmission, while transient absorption signals appear as a negative differential transmission. The change in optical density ( $\Delta\text{OD}$ ) was then calculated for each position of the delay line by taking the negative logarithm of the differential transmission, so that in the data shown below, transient absorption signals have a positive  $\Delta\text{OD}$ , while transient bleach signals have a negative  $\Delta\text{OD}$ .

The three-pulse experiments that are the main focus of this paper differ from the two-pulse experiments in that the  $\sim 2000$ -nm re-excitation beam is also overlapped with the pump and probe beams in the sample. In most of our analysis, we are interested in how the dynamics observed in the two-pulse pump–probe experiment are altered by the application of the  $\sim 2075$ -nm re-excitation pulse (in other words, the change of the change in absorbance, or  $\Delta(\Delta\text{OD})$ ), which we will also refer to as the *difference signal*. One way to measure the difference signal is to subtract a pump–probe trace with the re-excitation pulse blocked from a pump–probe trace with the re-excitation pulse unblocked. This method has the disadvantage, however, that both the optical density of the sample and the laser intensity must be constant for the entire duration of both scans. An alternate method for measuring the difference signal is to place the mechanical chopper in the re-excitation beam rather than the pump beam. This provides a measure of the difference signal by direct normalization of the pump–probe dynamics with the re-excitation pulse on against those with the re-excitation pulse off but has the disadvantage of not providing access to the two-pulse pump–probe dynamics. We verified for several pump and probe wavelength combinations that the difference signal dynamics measured by both methods were identical. The only minor difference between the two methods is that, when chopping the re-excitation beam, we occasionally observed a pulse-width-limited coherence artifact. This artifact turned out to be useful in that it provided a precise way to determine the arrival time of the re-excitation pulse and thus the time origin of the difference signal. When chopping the re-excitation beam, we were able to remove the coherence artifact by subtracting the difference signal measured with the pump pulse blocked. All the difference signals presented in this paper that were measured by chopping the re-excitation beam were corrected in this manner.

For the three-pulse data presented below, we varied the polarization of the re-excitation beam relative to the pump beam but found no effect of the re-excitation polarization on the dynamics of the difference signals. This does not rule out the possibility, however, that polarization-dependent dynamics may still be occurring on time scales faster than our  $\sim 200$ -fs instrument resolution. For example, in our two-pulse pump–probe experiments, we are unable to observe the fast anisotropic bleaching dynamics recently measured in higher time resolution experiments by Ruhman and co-workers.<sup>25</sup>

The sodide samples were prepared by following the same procedures presented in our previous work,<sup>17–19,21</sup> which are a modification of the methods originally presented by Dye.<sup>26</sup> Briefly, we dissolved sodium metal in THF (or, for a few of the experiments discussed below, tetrahydropyran (THP) with the aid of a crown ether that complexes the sodium cation. To obtain sizable three-pulse signals, we used highly

(23) We note that the results of the 480-nm probe experiments presented here are essentially indistinguishable from those of the 490-nm probe experiments reported in ref 21.

(24) Because the fundamental wavelength of our laser system varied a few nanometers from day to day, our choice of 1250 nm for the signal wavelength from the OPA meant that the idler wavelength used for re-excitation could change on a daily basis by  $\pm 25$  nm. All the experiments presented here were perfectly reproducible for re-excitation wavelengths varying between  $\sim 2000$  and  $\sim 2100$  nm. Thus, in the text we report the average idler wavelength (2075 nm) employed for all the experiments presented here.

(25) Wang, Z.; Shoshana, O.; Ruhman, S. *Proceedings of the 12th International Conference on Ultrafast Phenomena*; Springer Series in Chemical Physics 66; Springer-Verlag: Berlin, 2001.

(26) Dye, J. L. *J. Phys. Chem.* **1980**, *84*, 1084.

concentrated samples (optical density at the absorption maximum  $\sim 3$  for a 1-mm path length), although we verified the reproducibility of the results for samples with different concentrations to ensure that dimerization or ion-pair effects did not alter the signal dynamics.<sup>17</sup> Typical difference signal sizes ranged from  $\Delta(\Delta OD) \approx 0.01$  for the suppression of the recombination of the immediate contact pairs to  $\Delta(\Delta OD) \leq 10^{-4}$  for the enhanced recombination of the solvent-separated contact pairs.

### III. The Spectroscopy and Dynamics of the Na<sup>-</sup> CTTS Reaction

The dynamics of CTTS reactions have been the subject of a great deal of current interest. For example, Bradforth and co-workers have performed an extensive investigation of the electron detachment and recombination processes of aqueous iodide.<sup>27</sup> These workers found that the solvent motions that promote electron detachment take place in under 200 fs, while the back ET reaction takes place on a very different time scale of tens of picoseconds.<sup>27</sup> The recombination dynamics of electrons detached from other aqueous species, such as [Fe(CN)<sub>6</sub>]<sup>4-</sup> (ref 28) or indole,<sup>29</sup> however, take place on an even wider variety of time scales. These observations serve to emphasize the importance of the local solvent structure and the details of the electron detachment process in determining the dynamics of solvated electron recombination reactions. Part of the reason we choose to focus on a nonaqueous CTTS reaction in this paper is that the solvent dynamics governing both the electron detachment and recombination are slow enough that they can be observed directly via ultrafast spectroscopy.

We have extensively studied the system of choice for this paper, the CTTS reaction of the sodium anion in tetrahydrofuran (THF), in previous work.<sup>17–19,21</sup> The dynamical picture of the electron ejection and recombination processes that emerged from our studies is summarized in Figure 1A. Photoexcitation of one of the 3s electrons on Na<sup>-</sup> to the CTTS excited state creates a p-like wave function that is bound not by the Na nucleus but by the surrounding solvent cavity. The solvent molecules respond to accommodate the new electronic wave function, which leads to the detachment of the excited electron. Work by Ruhman and co-workers has demonstrated that the CTTS absorption band of Na<sup>-</sup> (solid curve in Figure 2) is inhomogeneously broadened,<sup>25</sup> likely consisting of three nominally degenerate (and orthogonal) s  $\rightarrow$  p-like transitions that are split by the instantaneous locally asymmetric environment of the solvent. Excitation on the low-energy side of the band produces an excited-state wave function that is well confined within the original solvent cavity. The electron thus remains in the original solvent cavity even after the solvent relaxation causes detachment, creating an “immediate contact pair” that recombines in  $\sim 1$  ps (Figure 1A, left). Excitation on the high-energy side of the band, on the other hand, produces a larger excited-state wave function that does not fit well within the solvent cavity. This increased spatial extent leads to the possibility that the detached electron can localize one or more solvent shells away from the

parent sodium atom, producing either a “solvent-separated contact pair” or a free solvated electron and sodium atom (Figure 1A, right). In contrast to the immediate contact pairs, the e<sup>-</sup><sub>s</sub> in solvent-separated contact pairs have negligible wave function overlap with their geminate Na<sup>0</sup> partners, so that recombination can take place only when a significant solvent fluctuation breaks up the metastable local solvent structure to allow for wave function overlap. In THF at room temperature, these fluctuations occur infrequently, so that the back ET reaction takes place on a hundreds-of-picoseconds time scale.<sup>19</sup>

Figure 1B shows the results of a typical pump–probe experiment that monitors (via their  $\sim 2$ - $\mu\text{m}$  absorption) the population of electrons produced following 580-nm excitation of the sodide CTTS band as a function of time on a logarithmic scale. Electrons appear in  $\sim 700$  fs following the CTTS excitation, the result of the CTTS detachment process that we believe is rate-limited by translational motions of the first-shell solvent molecules that are necessary to accommodate the detached electron and newly created solvated sodium atom.<sup>19</sup> The detached electrons then disappear on several time scales, the result of the back ET reaction of the electrons with the nearby sodium atoms to re-form Na<sup>-</sup>. The initial rapid loss of population is due to the geminate recombination of electrons in immediate contact pairs, while the slower, smaller amplitude decay reflects the recombination of electrons in solvent-separated contact pairs. The fact that the population does not decay to zero at long times is due to free electrons that are located farther away than the second solvation shell, formed either by direct photodetachment with a high-energy photon (or two-photon absorption)<sup>18</sup> or by the dissociation of a solvent-separated contact pair. These free e<sup>-</sup><sub>s</sub> do not recombine diffusively (since, when they do eventually approach within one solvent shell of the sodium atom, they become trapped in a solvent-separated contact pair) and thus do not undergo back ET on the subnanosecond time scales considered here.<sup>18</sup>

The relative fraction of electrons that localize in immediate contact pairs, solvent-separated contact pairs, or as free electrons varies smoothly with the choice of wavelength used to excite the CTTS transition. The solid curve in Figure 2 shows the CTTS band of sodide,<sup>13,30</sup> which extends from the UV all the way to the near-IR. Excitation wavelengths shorter than 400 nm create mainly solvent-separated contact pairs and free electrons, while excitation wavelengths longer than 800 nm create an overwhelming majority of immediate contact pairs.<sup>17</sup> The distribution of electrons also can be varied by increasing the excitation intensity, the result of a significant two-photon absorption cross section for sodide at wavelengths redder than  $\sim 700$  nm. For example, high-intensity excitation at 780 nm can create a ratio of immediate to solvent-separated contact pairs similar to that obtained with low-intensity excitation with 600-nm photons.<sup>18,31</sup>

The dot–dashed and dashed curves in Figure 2 show the absorption spectra of the other important species in the sodide CTTS reaction, the solvated electron<sup>8</sup> and solvated sodium atom<sup>32</sup> in THF, respectively. The large optical separation and

- (27) Kloepfer, J. A.; Vilchiz, V. H.; Lenchenkov, V. H.; Bradforth, S. E. *Chem. Phys. Lett.* **1998**, *298*, 120. Kloepfer, J. A.; Vilchiz, V. H.; Lenchenkov, V. A.; Germaine, A. C.; Bradforth, S. E. *J. Chem. Phys.* **2000**, *113*, 6288. Vilchiz, V. H.; Kloepfer, J. A.; Germaine, A. C.; Lenchenkov, V. A.; Bradforth, S. E. *J. Phys. Chem. A* **2001**, *105*, 1711.
- (28) Lenchenkov, V.; Kloepfer, J.; Vilchiz, V.; Bradforth, S. E. *Chem. Phys. Lett.* **2001**, *342*, 277.
- (29) Peon, J.; Hess, G. C.; Pecourt, J.-M. L.; Yuzawa, T.; Kohler, B. *J. Phys. Chem. A* **1999**, *103*, 2460.

- (30) Seddon, W. A.; Fletcher, J. W. *J. Phys. Chem.* **1980**, *84*, 1104.
- (31) Martini, I. B.; Schwartz, B. *J. Chem. Phys. Lett.* **2002**, in press.
- (32) The absorption spectrum of the THF-solvated Na atom was provided by John Miller. See also: Piotrowiak, P.; Miller, J. R. *J. Am. Chem. Soc.* **1991**, *113*, 5086. Bockrath, B.; Dorfman, L. M. *J. Phys. Chem.* **1975**, *79*, 1509. Bockrath, B.; Dorfman, L. M. *J. Phys. Chem.* **1973**, *77*, 1002.

**Table 1.** Summary of the Three-Pulse Experiments Monitoring the CTTS Dynamics of Na<sup>-</sup> Presented in Figures 3–9

pump wavelength (nm)	probe wavelength (nm)	species probed <sup>a</sup>	time second pulse is applied (ps)	contact pair re-excited <sup>b</sup>	probe time window <sup>c</sup>	effect on recombination <sup>d</sup>	relevant figure(s)
780	1250	e <sup>-</sup> abs.	0.2, 2.3	imm.	short	suppress	3A; 4A
780	480	Na <sup>-</sup> bleach	0.9, 1.5	imm.	short	suppress	3B; 4B
780	1250	e <sup>-</sup> abs.	0.2, 2.3	imm.	long	suppress	6
780	480	Na <sup>-</sup> bleach	0.9, 1.5	imm.	long	suppress	6
780	1250	e <sup>-</sup> abs.	5.9	solv-sep.	short	enhance	7A,C; 8C
780	480	Na <sup>-</sup> bleach	6.1	solv-sep.	short	enhance	7B,D; 8D
780	1250	e <sup>-</sup> abs.	5.9	solv-sep.	long	suppress	8A
780	480	Na <sup>-</sup> bleach	6.1	solv-sep.	long	suppress	8B
390	1250	e <sup>-</sup> abs.	3.5	solv-sep.	short	enhance	9
390	1250	e <sup>-</sup> abs.	~500	solv-sep. and free	short	enhance	9

<sup>a</sup> All the experiments probe either the transient absorption (“abs.”) of the CTTS-detached solvated electron or the bleach of the ground-state sodide anion.

<sup>b</sup> The arrival time of the 2075-nm pulse determines whether it predominantly re-excites electrons in immediate contact pairs (“imm.”), solvent-separated (“solv-sep.”) contact pairs, or free solvated electrons. <sup>c</sup> Probe time window refers to the time scale investigated in the experiment: “short” for scans of less than 10-ps duration and “long” for dynamics on the hundreds-of-picoseconds time scale. <sup>d</sup> The 2075-nm re-excitation pulse alters the recombination dynamics either by enhancement (“enhance”) or suppression (“suppress”) of the back electron-transfer reaction (see text for details).

convenient visible/near-IR location of the absorption spectra allow each of these species to be monitored independently during the course of the CTTS detachment and back ET dynamics.<sup>19</sup> For example, the back ET rate can be monitored by the recovery of the bleach of the sodide CTTS band in the visible (we typically probe at 480 nm) as well as by measuring the decay of the e<sup>-</sup><sub>s</sub> absorption near 2000 nm (as shown in Figure 1B). The dynamics of the solvated Na<sup>0</sup> also can be observed cleanly in the near-IR at wavelengths around 1100 nm. In addition, we know that, prior to the electron detachment, the CTTS excited state (Na<sup>-\*</sup>) is characterized by a sodium atom core absorption in the visible near 590 nm (the Na D line)<sup>17</sup> and a weak excited-state absorption in the near-IR around 1250 nm (not shown in Figure 2).<sup>33</sup> With the spectroscopy of all the species in this system characterized, we turn next to demonstrate how we can use a sequence of ultrashort laser pulses to modify the outcome of the CTTS reaction and thereby elucidate the details of the solvent motions governing ET.

#### IV. Controlling the CTTS Reaction of Sodide with Femtosecond Laser Pulses

Once the electron detachment process is started with a laser pulse tuned to the Na<sup>-</sup> CTTS band, the subsequent back ET dynamics can be modified using a second pulse that excites the e<sup>-</sup><sub>s</sub>. In our preliminary report,<sup>21</sup> we used a 780-nm pump pulse (pulse 1 in Figure 2) to create a distribution of detached electrons with the majority residing in immediate contact pairs. After allowing the CTTS dynamics to proceed for a desired length of time, we then applied a second, re-excitation pulse at ~2000 nm (pulse 2 in Figure 2) to alter the wave function of the newly detached solvated electron. By applying this second pulse within a few picoseconds of the initial excitation, we could ensure that the majority of the re-excited electrons were in immediate contact pairs (cf. Figure 1B). Application of the re-excitation pulse at later times, after the recombination of immediate contact pairs was complete, allowed selective excitation of only the long-lived solvent-separated contact pairs and free e<sup>-</sup><sub>s</sub>. We then probed the extent of the back ET reaction with a third pulse at 490 nm (pulse 3B in Figure 2) that measured the rate at which Na<sup>-</sup> was regenerated by monitoring the recovery of the bleached sodide CTTS band.<sup>21</sup> We found

that, when applied at early times, the re-excitation pulse shut off the fast component of the bleach recovery, indicating suppression of the rapid back ET reaction of the electrons in immediate contact pairs. On the other hand, application of the re-excitation pulse at later times to the electrons in solvent-separated contact pairs resulted in a dual behavior: the recombination reaction was enhanced at short times and suppressed at long times.<sup>21</sup>

In this section, we examine this multipulse manipulation of the sodide CTTS reaction in greater detail. In addition to monitoring the effects of the re-excitation pulse on the sodide bleaching dynamics at 480 nm,<sup>23</sup> we also examine the effects of re-excitation on the absorption dynamics of the solvated electron at 1250 nm (pulse 3A in Figure 2). A summary of all the three-pulse experiments discussed in this paper is presented in Table 1. We find that the 480- and 1250-nm probe data provide a consistent description of the re-excitation dynamics, and that the electron bleaching dynamics observed at 1250 nm offer a way to internally calibrate the fraction of solvated electrons that are re-excited. This, in turn, allows us to calculate the fraction of re-excited e<sup>-</sup><sub>s</sub> that relocalize and therefore the rates at which recombination and relocalization occur. All these results provide direct insight into the nature of the solvent motions that govern electron-transfer reactions and are consistent with a picture in which the translational motions of the one or two closest solvent molecules are critical in determining the final product of the electronic relaxation.<sup>19,34</sup> We note that Wasielewski and co-workers have performed similar three-pulse experiments on an organic donor–acceptor complex and were successful in controlling the position of the electron,<sup>35</sup> although spectral congestion in their organic complex did not allow detailed access to the molecular motions driving the electron-transfer reaction.

##### A. Re-excitation of Electrons in Immediate Contact Pairs.

The solid curves in Figure 3 present the results of standard two-pulse pump–probe experiments on Na<sup>-</sup> in THF with the pump pulse tuned to 780 nm. The lower panel shows the results obtained using a 480-nm probe pulse; the instrument-limited appearance of a negative change in absorbance (bleach) indicates

(34) Aherne, D.; Tran, V.; Schwartz, B. J. *J. Phys. Chem. B* **2000**, *104*, 5382. Tran, V.; Schwartz, B. J. *J. Phys. Chem. B* **1999**, *103*, 5570.

(35) See, e.g.: Debreczeny, M. P.; Svec, W. A.; Marsh, E. M.; Wasielewski, M. R. *J. Am. Chem. Soc.* **1996**, *118*, 8174. Lukas, A. S.; Bushard, P. J.; Wasielewski, M. R. *J. Am. Chem. Soc.* **2001**, *123*, 2440.

(33) Barthel, E. R.; Martini, I. B.; Keszei, E.; Schwartz, B. J., manuscript in preparation.

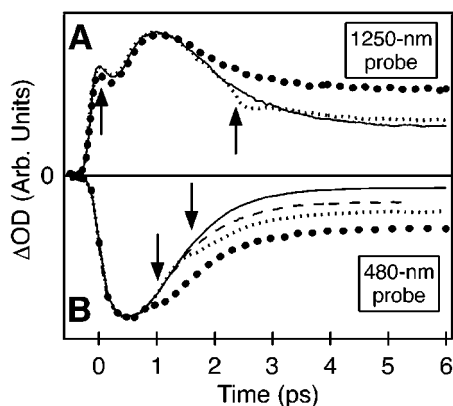


**Figure 3.** Comparison of two- and three-pulse experiments in which the  $\text{Na}^-$  CTTs band in THF is excited at 780 nm. The solid curves show the results of two-pulse experiments with the probe pulse tuned either to monitor the electron absorption at 1250 nm (panel A) or to examine the sodide bleach at 480 nm (panel B). The arrows mark the temporal arrival of the  $\sim 2075$ -nm re-excitation pulse for different three-pulse experiments; the three-pulse data are shown as the various dotted and dashed curves. Except for the left-most arrow and large-dotted curve in panel A, in which the re-excitation pulse arrives during the electron detachment process, the delay times for the re-excitation pulses in these experiments were chosen to arrive during the recombination of immediate contact pairs. The dashed and small-dotted curves in panel B were generated with re-excitation pulses at the same delay time but with different intensities.

that the 780-nm excitation instantaneously depletes the ground-state population of sodide. After the electron detachment, the 480-nm absorption recovers in a few picoseconds as  $\text{Na}^-$  is regenerated by the recombination of immediate contact pairs. The small offset indicates that some electrons still have not recombined into  $\text{Na}^-$  after 5 ps, indicating that, while most of the detached electrons were localized in immediate contact pairs, the 780-nm excitation pulse also produced a small fraction of electrons in long-lived solvent-separated contact pairs.<sup>18</sup>

The upper panel of Figure 3 shows complementary results with the probe pulse tuned to 1250 nm; the dynamics of this signal are more complex than those of the 480-nm bleach, and our assignment of the features in this signal will be discussed in detail elsewhere.<sup>33</sup> Briefly, the instrument-limited rise is attributed to absorption from the instantaneously created CTTs excited state ( $\text{Na}^{-*}$ ). On the basis of the work of Ruhman and co-workers<sup>25</sup> and a simple fit of the  $\text{Na}^-$  absorption spectra to the sum of three Gaussians,<sup>33</sup> we expect the transition between the lowest and highest p-like CTTs excited states to occur in this spectral region. This absorption is weak because it would be symmetry forbidden (a  $p \rightarrow p$  transition) in the absence of the locally asymmetric solvent environment. Once the solvent molecules surrounding the excited state begin to move, both the energy and oscillator strength of this transition change, leading to the observed initial rapid decay of the absorption.<sup>36</sup> The subsequent rise of the signal is a signature of the  $\sim 700$ -fs electron detachment process, resulting from the fact that the  $e^-_s$  has a weak 1250-nm absorption with cross section similar

(36) It should be possible to make a detailed analogy between the transient spectroscopy of the  $\text{Na}^-$  CTTs band and that of the hydrated electron. Both species consist of an s-like ground-state wave function with three quasi-degenerate p-like excited-state wave functions whose energy is split by the locally asymmetric solvent environment. Mixed quantum-classical MD simulations on the spectroscopy of the photoexcited hydrated electron indicate that small solvent motions can dramatically alter the symmetry and thus the oscillator strength of the nearly forbidden low-p-to-high-p transition. See, e.g.: Schwartz, B. J.; Rossky, P. J. *J. Chem. Phys.* **1994**, *101*, 6917.

to that of  $\text{Na}^0$  (cf. Figure 2). The absorption signal then decays on the same  $\sim 1$ -ps time scale as the 480-nm bleach, reflecting the disappearance of the electrons in immediate contact pairs as they recombine to regenerate  $\text{Na}^-$ . The offset of the 1250-nm signal is larger than that of the 480-nm bleach because the small signal size at 1250-nm required the use of higher pump intensities, leading to a small two-photon absorption component that produced a higher fraction of solvent-separated contact pairs and free electrons.

**1. The Effect of Re-excitation on the Back ET of Immediate Contact Pairs.** The dashed and dotted curves in both panels of Figure 3 show the dynamics when the  $\sim 2075$ -nm re-excitation pulse is applied to the immediate  $e^-_s:\text{Na}^0$  contact pairs at various delay times indicated by the arrows and summarized in Table 1. The dashed curve in the lower panel shows a 480-nm probe experiment with the  $\sim 2075$ -nm pulse applied at 1.5 ps, the same delay time as the small dotted curve, but using a re-excitation pulse with lower intensity. In both panels, it is clear that the net effect of the re-excitation pulse is to produce a larger long-time offset compared to that of the corresponding two-pulse experiment. This indicates that, following  $\sim 2075$ -nm re-excitation, there are more  $e^-_s$  (and correspondingly less regenerated  $\text{Na}^-$ ) present than there would have been without re-excitation; thus, we refer to these types of traces as *recombination-suppression* signals. We will argue below that this recombination suppression is a consequence of producing a redistributed electron population that has a larger fraction of solvent-separated contact pairs and free electrons. In addition, the 1250-nm electron absorption traces in Figure 3A show an initial dip in the three-pulse traces (dotted curves) that is absent in their  $\text{Na}^-$  bleaching counterparts in Figure 3B. This feature is due to bleaching of the  $e^-_s$  ground-state absorption by the  $\sim 2075$ -nm re-excitation pulse. The depleted ground-state electron population recovers quickly as the re-excited, delocalized electrons in the conduction-band relocalize into solvent cavities and relax back into their ground states.

Figure 4 shows the recombination-suppression difference signals for the same experiments presented in Figure 3. Figure 4A presents the difference signal for the 1250-nm probe experiment when the re-excitation pulse is applied 2.3 ps after the pump pulse (small dotted curve in Figure 3A). The negative feature at early times in this trace is the ground-state bleach of the electron. The fact that the difference signal turns positive in under 2 ps reflects both the difference in recombination dynamics caused by the re-excitation pulse and the finite excited-state lifetime of the re-excited electrons. We will show in a future publication that these two effects can be separated, allowing both the altered recombination dynamics and the electron excited-state relaxation to be studied independently; in particular, we find that free  $e^-_s$  have the same excited-state lifetime as electrons trapped in either immediate or solvent-separated contact pairs.<sup>31</sup> Figure 4B shows the difference signal for each of the three 480-nm probe experiments presented in Figure 3B, although the time origin of the re-excitation pulse has been shifted and the three traces were normalized to the same maximum amplitude for better comparison. The dot-dashed curve in Figure 4B shows the experimentally measured instrument response, demonstrating clearly that the rise of the difference signals is resolved. The three traces are identical within our experimental precision, including the two experiments

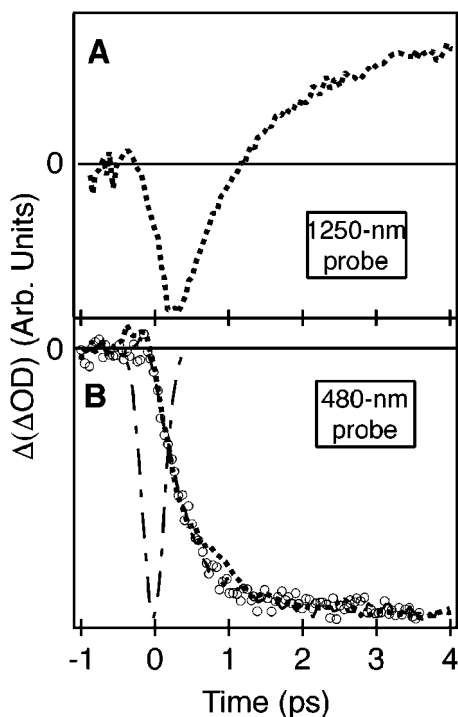


**Figure 4.** Difference signals for some of the three-pulse data presented in Figure 3. (A) Difference signal for the 780-nm pump/2075-nm re-excitation/1250-nm probe experiment in which the re-excitation pulse arrives at a delay of 2.3 ps (small-dotted curve in Figure 3A). (B) Difference signals for the 780-nm pump/2075-nm re-excitation/480-nm probe experiments shown in Figure 3B; the three difference signals have been normalized to the same maximum height and shifted temporally to the same relative arrival time of the re-excitation pulse. The dot-dashed curve shows the instrument response (cross-correlation between the 2075-nm re-excitation and 480-nm probe pulses).

with the same time origin but different re-excitation pulse intensities. This lack of intensity dependence suggests that our measured difference signals result from one-photon absorption of the re-excitation pulse and that multiphoton absorption does not play an important role in the observed dynamics.

The difference signals in Figure 4B provide a window on what happens at the molecular level after a  $\sim 2075$ -nm photon is absorbed by an immediate contact-pair electron. These difference signals are a measure of the amount of sodide that the  $\sim 2075$ -nm re-excitation pulse prevents from being regenerated through the back ET reaction. The resolved rise of the difference signal shows that suppression of the electron recombination is not instantaneous: the back ET reaction is not immediately shut off upon excitation of the electron. This slow rise cannot be related to solvation dynamics or local heating induced by the re-excitation pulse because the difference signal measures only sodide anions that have *not* been created. Instead, the delayed rise of the difference signal must be due to a photoinduced change in the reactivity of the  $e^-_s$ . The results of Barbara and co-workers<sup>11</sup> suggest that the diffuse excited state of the electron can still undergo the back ET reaction with a rate dependent on the amount of overlap of the excited wave function with the  $\text{Na}^0$  acceptor. A change in the back ET rate from the excited state would produce sodium anions on a different time scale than if they would have been produced without the re-excitation pulse. This difference between the back ET rates of the ground and excited states could potentially explain the observed rise of the difference signal.

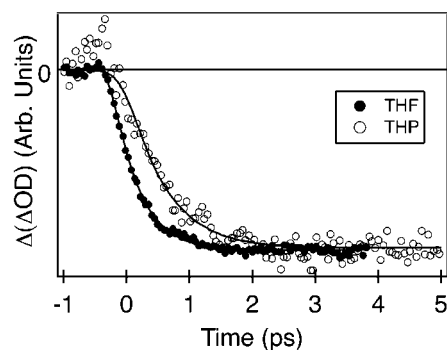


**Figure 5.** 780-nm pump/ $\sim 2075$ -nm re-excitation difference signals monitoring the sodide bleaching dynamics at 480 nm in two different solvents: THF (solid circles; same as thin dashed curve in Figure 4B) and THP (open circles).

Even given that recombination with a different rate is possible from the excited state, it is still not obvious how to explain the fact that the difference signal rises but does not subsequently decay. If the excited electrons could relax back to their ground states only in their original solvent cavities, then we would expect the difference signal to reach a maximum at time zero, when the most electrons were in the excited state. The difference signal would then decay back toward zero at longer times after all the excited-state electrons had relaxed back to their ground states. The experimental traces in Figure 4, however, show a very different behavior. The only way to explain the data in Figure 4 is to assume that the re-excitation pulse ultimately produces a new species that has a lower recombination rate than both ground- and excited-state electrons. The most logical possibilities for this new species are ground-state electrons in solvent-separated contact pairs or free ground-state  $e^-_s$ , suggesting that re-excitation produces a *relocalization* of the electron into a new solvent cavity. Thus, the rise of the difference signals in Figure 4 is not simply related to the difference in ground- and excited-state recombination rates, but also must depend on the rate at which the excited electrons undergo relocalization.

To further investigate the origin of the rise of the difference signals in Figure 4, we present three-pulse recombination-suppression difference signals for the sodide back ET reaction in two different solvents, THF and tetrahydropyran (THP, a six-membered cyclic ether similar to THF) in Figure 5. We recently completed a full set of two-pulse sodide CTTS experiments in a variety of different solvents, including THP.<sup>33</sup> A detailed analysis of the CTTS dynamics found that both the photodetachment and back ET reactions in THP are  $\sim 1.5$  times slower than those in THF. In other words, the molecular motions of the solvent that promote electron detachment from the CTTS excited state are  $\sim 50\%$  slower in THP than in THF, consistent with the fact that the THP molecules undergo slower translational motions.<sup>33</sup> The data in Figure 5 were taken using a 480-nm probe wavelength: the solid circles are the same data in THF shown as the thin dashed curve in Figure 4B, the open circles represent the data in THP, and the solid curves are fits to the data of a single-exponential rise plus an offset. The rise of the difference signal in THP fits best to a  $700 \pm 100$  fs exponential, which is almost exactly a factor of 1.5 greater than the rise time observed in THF,  $450 \pm 100$  fs. Since the rate of recombination from the excited state should depend only on the degree of overlap of a highly delocalized wave function,



we would expect it to be the same in both THF and THP. Thus, the 50% difference we observe between the two solvents means that the rise of the difference signal is due primarily to the rate for the excited-state electron to relocalize. This implies that the rate of back ET from the excited state must be comparable to that from the ground state, or about  $1 \text{ ps}^{-1}$  in THF.<sup>37</sup> The strong solvent dependence also suggests that the  $\text{Na}^0$  in the immediate pair does not play a major role in the relaxation and relocalization of the re-excited electron. The fact that both the electron detachment and relocalization processes are slower by the same ratio in THP relative to THF suggests that the same types of solvent motions are responsible for both detachment and relocalization. We will return to this question of the solvent motions controlling relocalization in section IV-B below, where we will show that, in both THF and THP, the electron bleach recovery rate matches the rate of relocalization measured in Figure 5.

How efficient is the relocalization of excited immediate contact-pair electrons into different solvent cavities? Using the 1250-nm probe experiments presented in Figures 3A and 4A, we can estimate the relative fractions of electrons that either relocalize into different solvent cavities or relax into their original cavities. The idea is that the magnitude of the electron bleach signal is proportional to the total number of re-excited electrons, but the suppressed recombination signal is proportional only to the number of electrons that relocate. Of course, not all of the electrons that are re-excited are in immediate contact pairs, but we can estimate the fraction of electrons that are in immediate pairs at the time of re-excitation from the two-pulse experiment (solid curve) in Figure 3A. This fraction is  $\sim 50\%$  for re-excitation at 2.3 ps (small dotted curve). After deconvolving the instrument response, we can then scale the amplitude of the bleach signal (the negative early-time peak in Figure 4A) by the fraction of electrons in immediate contact pairs and compare the result to the magnitude of the positive recombination-suppression signal (long-time positive offset in Figure 4A). Finally, a glance at Figure 2 shows that the absorption cross section of  $\text{Na}^0$  at 1250 nm is comparable to that of the solvated electron. Thus, we also need to correct the magnitude of the recombination-suppression signal for the “extra” absorption of the  $\text{Na}^0$  atoms whose recombination is also suppressed (note that  $\text{Na}^0$  is not bleached by the 2075-nm re-excitation). When all these corrections are accounted for in the dotted trace in Figure 3A, this analysis indicates that 35% of the re-excited immediate contact-pair electrons relocalize into either solvent-separated contact pairs or free electrons. A similar analysis on multiple experiments gives a relocalization quantum yield of  $0.3 \pm 0.1$ .

The calculated  $\sim 0.3$  quantum yield for relocalization makes it clear that the rates of electron relaxation into the original cavity and electron relocalization into a new solvent cavity must be quite similar. This similarity is not surprising because similar

(37) This means that the net overlap of the ground- and excited-state wave functions of the electron with the sodium atom must be quite similar. Our picture for this is based in Figure 1: in the immediate-pair ground state, the sodium atom sits in the first solvent shell of the electron. Thus, even though the electron density in the cavity is high, the net overlap is not perfect because the sodium atom lies at the outskirts of the ground-state wave function. Excitation leads to delocalization that lowers the electron density within the solvent cavity but also allows the lower-density excited-state wave function to completely engulf the sodium atom. Thus, we believe that the density decrease upon excitation is roughly balanced by the improvement in wave function contact, leading to similar reaction rates for both electronic states.

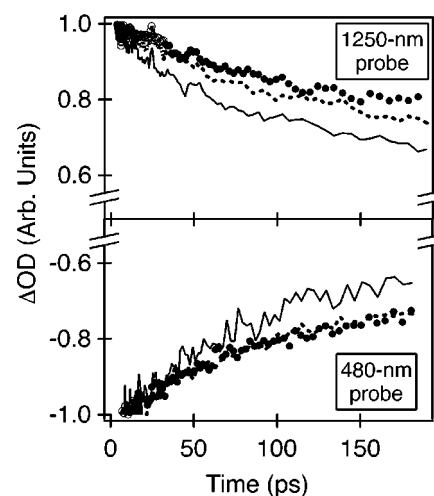


**Figure 6.** Long-time dynamics of the two- and three-pulse experiments presented in Figure 3; the symbols are the same as in Figure 3 (the dashed trace in Figure 3B has been omitted for clarity). Each trace has been normalized to the same amplitude at 8-ps delay. Note that the y-axis has been expanded to better show the subtle differences between the experiments.

solvent motions must be involved in the relaxation of the excited-state electron, regardless of whether it relocalizes into a new cavity. The sudden expansion of the wave function upon re-excitation reduces the electron density in the original cavity, therefore reducing the repulsive forces between the electron and first-shell solvent molecules. We believe that the predominant driving force for relaxation is the translational motions of the one or two closest solvent molecules toward the center of the cavity.<sup>19,34</sup> The solvent translations around the re-excited electron can create new holes in the solvent structure that are located one or more solvent shells away from the sodium atom. Thus, when the electron relaxes back to its ground state, there is a significant probability that the largest available cavity for relocalization is not the original cavity containing the  $\text{Na}^0$ , but a cavity some distance away. The fact that the rise of the difference signal presented in Figure 4B is comparable to (although slightly faster than) the CTTS photodetachment time supports our idea that similar solvent motions are responsible for both electron detachment and relocalization.

**2. The Fate of Electrons Re-excited from Immediate Contact Pairs.** As summarized in Table 1, Figure 6 presents the same traces shown in Figure 3, but on a hundreds-of-picoseconds time scale. Each of the traces in Figure 6 has been normalized to have the same amplitude at 8 ps, a time at which all the immediate contact-pair electrons (both those produced by the original pump pulse and those that were re-excited and happened to relocalize into their original solvent cavities) have recombined. This amplitude scaling thus allows us to directly compare the long-time decay dynamics of the original CTTS-detached electrons to those of the re-excited electrons. The data show a slower decay rate and higher offset for the three-pulse experiments (dotted curves) relative to the two-pulse experiment (solid curve), suggesting that re-excitation increases the fraction of free electrons remaining at long times. In our previous work, we saw a decreased long-time decay rate and larger offset in two-pulse pump–probe experiments when the CTTS excitation energy was increased, a signature of an increase in the number of free electrons relative to those trapped in solvent-separated contact pairs.<sup>17,18</sup> Thus, Figure 6 suggests that the energy

provided by re-excitation acts similarly to the excess energy provided by changing the CTTS pump wavelength in controlling the distribution of free electrons and solvent-separated pairs.

This idea becomes even more apparent when considering a three-pulse experiment in which the re-excitation pulse arrives at very early times, such as the data represented by the large dotted curve in Figure 3A, in which the re-excitation pulse is applied at 0.2 ps. In this experiment, the  $\sim 2075$ -nm re-excitation pulse arrives during the decay of the CTTS excited state, a time when most of the CTTS-excited electrons have not yet been ejected. Thus, we would expect the distribution of solvent-separated contact pairs and free electrons to be determined by the sum of the energies of the pump (780 nm) and re-excitation (2075 nm) pulses. Indeed, the long-time decay of the difference signal corresponding to the large dotted curve in Figure 6 matches well to that of a regular two-pulse experiment in which the initial pump pulse is tuned to  $\sim 570$  nm (not shown).<sup>38</sup> This implies that, as long as the electron has not yet detached, the combination of separate pump and re-excitation photons produces the same detachment dynamics as a single photon whose energy is the same as the sum of the pump and re-excitation photons.<sup>39</sup> If the re-excitation pulse is applied at a later time, such as in the small-dotted traces in Figure 6, however, it will excite already-detached electrons that have (at least partially) thermally equilibrated with the surrounding solvent. This means that part of the energy delivered by the re-excitation pulse will have to overcome a solvation barrier in order to redistribute the electrons into different solvent cavities. Indeed, the long-time decays seen in the small-dotted curves in Figure 6 indicate that the re-excitation pulse produces fewer solvent-separated contact pairs and free electrons when applied after the electrons have detached than if applied before the electrons have detached. Thus, the solvent motions following CTTS detachment create a stable solvent cavity for the ejected e<sup>-</sup>, that requires a significant amount of energy to disrupt.

In principle, we could estimate the magnitude of the solvation energy barrier by a careful analysis of the long-time decay dynamics of three-pulse experiments in which the electron was re-excited at different delay times or with different re-excitation pulse wavelengths. However, a number of experimental difficulties have prevented this kind of analysis from producing meaningful results. First, the difference in the long-time dynamics for similar excitation energies is so small that it is

(38) We noted in ref 21 that a two-pulse experiment with a 560-nm pump shows the same long-time decay dynamics as a three-pulse 780/2000/490-nm experiment; this result turns out to be a coincidence. A better comparison would have been between the 560-nm pump two-pulse experiment and the three-pulse difference signal. When we do compare the three-pulse difference signals, it becomes apparent that there is indeed dissipation when the re-excitation pulse is applied at longer ( $\geq 1$  ps) times.

(39) The fact that the re-excitation pulse energy is additive during the first 0.1–0.3 ps implies that the electron has not yet been ejected and that little dissipation has taken place, contrary the assertions of Ruhman and co-workers (Wang, Z.; Shoshana, O.; Hou, B.; Ruhman, S., submitted). In our opinion, the relatively long ( $\sim 700$  fs) CTTS excited-state lifetime is not surprising for two reasons. First, the lifetimes of related species occur on this same time scale, even in solvents whose relaxation is much faster than that of THF, such as water. For example, the CTTS excited-state lifetime of aqueous I<sup>-</sup> has been measured at 200 fs,<sup>27</sup> despite the presence of a sub-50-fs inertial relaxation in liquid water. Second, the CTTS excited state of Na<sup>-</sup> should be p-like in nature, while that of the ejected electron is s-like in nature. This means that, unlike the CTTS excitation of iodide, a symmetry-changing nonadiabatic transition must take place before the electron can be ejected from excited sodide. Such symmetry-altering transitions also must take place in the relaxation of the hydrated electron, which is known to occur on the 300–500-fs time scale.<sup>11</sup> In combination with the additivity of the re-excitation pulse energy when applied at early times, all these reasons lead us to believe that a 700-fs CTTS lifetime is quite reasonable for sodide.

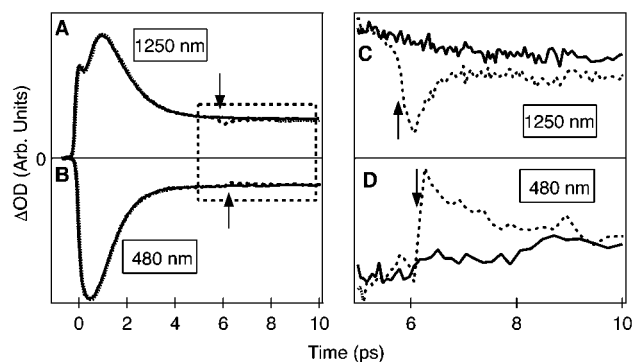


**Figure 7.** Comparison of two- and three-pulse experiments for re-excitation of the electrons in solvent-separated contact pairs. The Na<sup>-</sup> CTTS band in THF is excited at 780 nm, and the re-excitation pulse is applied at a delay of  $\sim 6$  ps, after the recombination of immediate contact pairs is complete. The solid curves show the two-pulse experiments, while the dotted curves represent the three-pulse data; the arrows mark the temporal position of the 2075-nm re-excitation pulse. Panels A and B show the 1250-nm electron absorption and 480-nm sodide bleaching dynamics, respectively. Panels C and D show an expanded view of the data inside the dashed box in panels A and B.

extremely hard to distinguish closely decaying traces (note the expanded y-axis scale in Figure 6). Second, the substantial two-photon absorption cross section of sodide at 780 nm means that small variations in the pump pulse energy can alter the fraction of free electrons in the initial distribution,<sup>18</sup> masking subtle long-time effects produced by the re-excitation pulse.<sup>40</sup> Finally, both our laser system and the sample provide restrictions on the range of experiments that can be done with different re-excitation wavelengths. For example, there is considerable two-photon absorption of the re-excitation pulse at wavelengths to the blue of 2000 nm, and our laser cannot produce sufficient energy to create re-excitation pulses to the red of  $\sim 2250$  nm. We are presently carrying out experiments to explore this question of the size of the solvation energy barrier by studying the long-time recombination dynamics as a function of sample temperature.

We close this section by noting that Figure 6 also shows that the long-time recombination of the immediate contact pairs is not completely suppressed by the re-excitation pulse. The fact that the difference signals decay on the hundred-of-picoseconds time scale is a signature that most of the re-excited electrons have relocalized into solvent-separated contact pairs. This implies that the delocalization of the excited electron's wave function is not large enough to access the bulk of the solvent with high probability; in other words, most of the time the effect of the  $\sim 2075$ -nm re-excitation is to relocalize the electron only into a neighboring solvent cavity. This idea opens the possibility of using re-excitation to take an electron in a solvent-separated contact pair and relocalize it into the neighboring solvent cavity containing the sodium atom. We study exactly this possibility in the next section.

### B. Re-excitation of Electrons in Solvent-Separated Contact Pairs.

Figures 7 and 8 show the results of both two-pulse (solid

(40) We note that even a small amount of two-photon excitation can alter the long-time relaxation following the initial 780-nm pump, making it difficult to study subtle changes in the long-time decay of the difference signals. This sensitivity of the long-time dynamics to tiny changes in the excitation conditions, in combination with the intrinsically poor signal-to-noise ratio of the three-pulse experiment, is what prevents us from obtaining a more quantitative understanding of the energy dissipation following CTTS excitation.

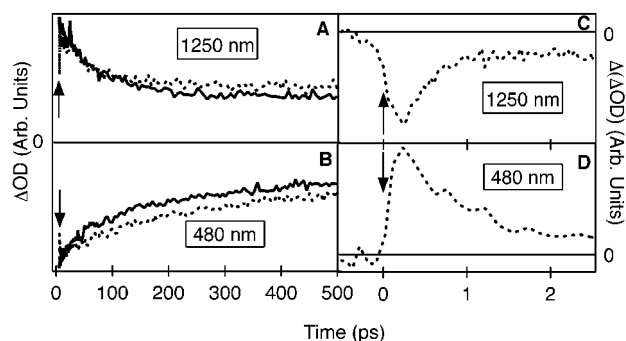


**Figure 8.** Panels A and B show the long-time dynamics of the data presented in Figure 7A and B, respectively. Panels C and D show the difference signals for the short-time data presented in Figure 7C and D, respectively. The arrows show the arrival of the  $\sim 2075$ -nm re-excitation pulse.

curves) and three-pulse (dotted curves) experiments in which the re-excitation pulse was applied  $\sim 6$  ps after the pump pulse and the dynamics were probed at both 480 nm (panels B and D) and 1250 nm (panels A and C), as summarized in Table 1. The long delay between the pump and re-excitation pulses guarantees that any immediate contact pairs produced by the pump pulse have recombined before the re-excitation pulse is applied. The 780-nm pump wavelength produces few free  $e^-$ s, so the re-excitation pulse in these experiments acts primarily on electrons in solvent-separated contact pairs. The first few picoseconds of the two- and three-pulse signals are presented in Figure 7A and B (and shown on an expanded scale in Figure 7C and D), while Figure 8A and B shows the same data on a hundreds-of-picoseconds time scale. The short-time difference signals corresponding to the data in Figure 7C and D are shown in Figure 8C and D. For the 1250-nm data in Figure 8C, the negative difference signal corresponds to a loss of electron absorption, while the positive  $\Delta(\Delta OD)$  at 480 nm in Figure 8D corresponds to an increased absorption from  $\text{Na}^-$ .

In keeping with our preliminary work in ref 21, we attribute the increased amount of  $\text{Na}^-$  in Figures 7D and 8D and decreased number of electrons in Figures 7C and 8C to a rapid enhancement in the rate of solvent-separated back ET caused by the re-excitation pulse. Because  $\text{Na}^-$  is the only species in this system that can absorb light at 480 nm, the decay of the 480-nm difference signal in Figure 8D must be due to solvation dynamics.<sup>41</sup> The decreased amount of  $\text{Na}^-$  at long times in Figure 8B and corresponding increase in the number of  $e^-$ s at long times in Figure 8A, on the other hand, must reflect a long-time recombination suppression of solvent-separated contact pairs. This is consistent with the idea that the re-excitation pulse acts primarily to relocalize the solvent-separated contact-pair electrons. Some fraction of the re-excited electrons may relocalize into the adjacent solvent cavity containing the  $\text{Na}^0$ , thus providing a significant acceleration of the rate at which these electrons undergo recombination. The remaining re-excited electrons, however, will relocalize either into their original

(41) Since the enhanced recombination occurs instantaneously upon re-excitation of the electron, the surrounding solvent is out of equilibrium with the newly formed sodium anion; the relaxation of the solvent back to equilibrium shifts the  $\text{Na}^-$  spectrum past our 480-nm probe window, producing the apparent decay of the signal. Given that it takes  $\sim 700$  fs for the solvent to induce the forward electron transfer by rearranging around the initially photoexcited CTTs state, it is not surprising that it takes a similar amount of time to “undo” those solvent motions and re-establish equilibrium after the electron is placed back onto the sodium atom.

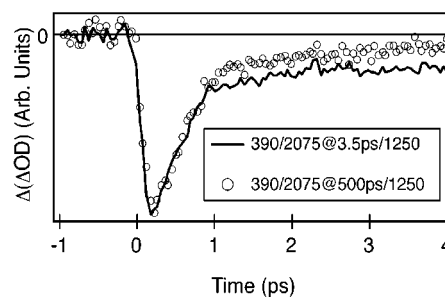


**Figure 9.** Difference signals for three-pulse experiments on the  $\text{Na}^-$  CTTs band in THF that use a 390-nm pump pulse,  $\sim 2075$ -nm re-excitation pulse, and 1250-nm probe pulse. The solid curve shows the data when the re-excitation pulse is applied 3.5 ps after the pump pulse, when the majority of the electrons are in solvent-separated contact pairs. The open circles show the results when the re-excitation pulse is applied  $\sim 500$  ps after the pump pulse, acting primarily on the free electrons that remain after most of the solvent-separated contact pairs have recombined. The data have been normalized to the same maximum amplitude and shifted to the same time relative to the arrival of the re-excitation pulse.

solvent cavities or into cavities even farther from the sodium atom, suppressing the recombination at longer times. We note that the initial loss and subsequent fast recovery seen at 1250 nm in Figures 7C and 8C is due to the excited-state relaxation of the electron, similar to what we observed in the previous section in Figures 3A and 4A. While the bleaching dynamics of the electron could, in principle, obscure the enhancement of the back ET at early times, the definite negative offset that persists for several picoseconds after this decay is complete confirms that the number of  $e^-$ s does indeed decrease following re-excitation.

To better understand the role of electron bleaching dynamics and confirm our assignments of the traces in Figures 7 and 8, we performed another three-pulse experiment in which the electrons were re-excited at a delay time long enough ( $\geq 500$  ps) that the recombination of solvent-separated pairs was nearly complete. Figure 9 compares the difference signals for this long-time re-excitation experiment (circles) with a shorter-time re-excitation experiment similar to that shown in Figure 8C (solid curve). For both traces in Figure 9, the pump pulse was tuned to 390 nm so that the initial distribution contained a larger fraction of solvent-separated contact pairs and free electrons, thus ensuring that there still would be a significant number of electrons remaining at 500 ps for re-excitation. The two traces in Figure 9 also have been normalized to the same maximum height, which corresponds to the same total number of re-excited electrons. The bleach and subsequent rapid ( $\sim 450$  fs) recovery of the electrons' absorption is similar in the two experiments, suggesting that the excited-state lifetimes of free electrons and electrons in solvent-separated contact pairs are similar.<sup>31</sup> More importantly, the comparison in Figure 9 also makes it clear that, for the same total number of re-excited electrons, re-excitation at earlier times leads to a larger recombination enhancement than re-excitation at later times. This implies that the number of electrons whose recombination is accelerated is proportional not to the total number of electrons re-excited, but instead to the fraction of re-excited electrons that were in solvent-separated contact pairs. Thus, Figure 9 helps to confirm that the 2075-nm re-excitation pulse enhances the recombination for solvent-separated electrons to a much greater extent than for free electrons. This is consistent with our conclusions in the previous section that re-excitation primarily causes relocalization into an

adjacent cavity rather than into the bulk of the solvent. This conclusion is also consistent with the fact that the long-time difference signals for the solvent-separated contact pairs do not decay on the hundreds-of-picoseconds time scale, indicating that the non-recombining species created upon re-excitation of solvent-separated pairs are free electrons. Finally, the fact that the 500-ps re-excitation still causes a small amount of recombination enhancement verifies that solvent-separated contact pairs are metastable species that live for hundreds of picoseconds, as suggested in Figure 1.

We mentioned in the previous section that the rise of recombination-suppression signals for the immediate contact pairs occurred on the same time scale as the electron bleach recovery. Indeed, both of the traces in Figure 9 can be fit well to a  $\sim 450$ -fs exponential decay plus an offset (fits not shown). We also found a similar agreement between the electron bleach recovery time and the rate of recombination suppression in THP. This means that the relaxation of electrons from the excited state and the relocalization of re-excited electrons represent two manifestations of the same process: electrons relocalize because they relax from their excited state. What types of solvent motions are responsible for this process? It is clear that translational solvent motions must be involved, because new solvent cavities must be created for the electron to relocalize. This reasoning is similar to arguments we have made in previous work concerning the initial production of the electron via CTTS detachment.<sup>19</sup> We believe that the CTTS detachment ( $\sim 700$  fs) takes a bit longer than electron relocalization ( $\sim 450$  fs) because CTTS photodetachment requires the creation of a completely new solvent cavity via the large-amplitude motion of many solvent molecules, while relocalization can occur when only one or two first-shell molecules move in toward the center of the electron's original solvent cavity (cf. Figure 1). This might also explain why relocalization of the electron tends to occur into an adjacent solvent cavity; the rate to form a completely new cavity in the bulk of the solvent is likely to be prohibitively slow.

Finally, we can use the magnitudes of the various features in the difference signals in Figures 7 and 8 to calculate the relative fraction of re-excited solvent-separated pairs that undergo enhanced recombination. This analysis, however, is partially obscured both by the electron bleach recovery dynamics at 1250 nm and by the  $\sim 2$ -ps decay in the 480-nm difference signal that we have assigned<sup>21</sup> to solvation dynamics associated with the cooling of the newly created hot Na<sup>-</sup>.<sup>41</sup> If we assume, however, that the flat offset of the 1250-nm difference signal (after the bleach recovery is complete) represents the entire extent of enhanced recombination, then we can estimate the fraction of solvent-separated pairs that undergo enhanced back ET from the data in Figure 8C. We can also estimate the fraction of solvent-separated pairs whose recombination is suppressed by the re-excitation pulse from the long-time data in Figure 8A and B. These assumptions give a ratio of suppressed to enhanced recombination for the re-excited solvent-separated pairs that is very roughly unity.<sup>42</sup> At first this ratio seems surprisingly low, since solid angle considerations would lead us to expect that there are many more ways for a re-excited solvent-separated

electron to relocalize farther from the sodium atom than into the same cavity with it; cf. Figure 1. However, we already determined in the previous section that the excited state of the solvated electron can undergo back ET with a  $\sim 1$  ps<sup>-1</sup> rate if the delocalized wave function completely overlaps the sodium atom.<sup>37</sup> Thus, the majority of the solvent-separated pair recombination enhancement results not from relocalization but from the enhanced overlap of the excited-state electron with the Na<sup>0</sup> one solvent shell away. This reasoning is roughly consistent with the data presented in the previous section. If the re-excited solvent-separated electrons undergo recombination at a  $\sim 1$  ps<sup>-1</sup> rate similar to their immediate-pair counterparts, then the 450-fs bleach recovery time (rate of  $\sim 2$  ps<sup>-1</sup>) predicts that the ratio of re-excited electrons that relocalize versus recombine should be roughly 2. This is reasonably close to the value of roughly unity determined from the data in Figure 8. Given that this argument does not account for the fraction of electrons that relocalize into the cavity with the sodium atom or for solvent-separated pairs that spontaneously dissociate, we consider the rough agreement using these rate constants to be satisfactory.<sup>42</sup>

## V. Conclusions

In summary, we have shown that it is possible to both study and control the dynamics of electron-transfer reactions in solution using a sequence of femtosecond laser pulses. The CTTS transition of Na<sup>-</sup> provides a perfect model system for investigating ET reactions. The spectrum of each of the species involved is well characterized and conveniently located in the visible and near-IR. Moreover, the entire system contains only electronic degrees of freedom, so that any spectroscopic changes that occur following excitation must result from motions of the solvent. In addition to providing a molecular-level window into solvent motions, the lack of congestion from vibrational or rotational degrees of freedom makes this system amenable to manipulation with femtosecond laser pulses without the need for special pulse shapes or phase-locking.<sup>21</sup> This ability to alter the electronic wave function at selected points during the course of the reaction provides new insights into how solvent dynamics control electron transfer.

Excitation of one of the 3s electrons of Na<sup>-</sup> into the CTTS band produces a p-like excited state that is bound only by the presence of the surrounding solvent cavity and not by the Na atom. The first-shell solvent molecules are out of equilibrium with the electronic excited state and respond with motions that eventually lead to detachment, so that the electron's center of mass no longer coincides with the sodium nucleus. This process takes  $\sim 700$  fs, a time we believe is rate-limited by both the nonadiabatic relaxation required to remove the node from the excited-state wave function and the translational solvent motions necessary to produce a new solvent cavity in which to accommodate the newly detached ground-state electron.<sup>39</sup> The CTTS excitation wavelength determines the spatial extent of the excited-state wave function, leading to detachment of the electron either into a solvent cavity that has the Na atom in its first shell or into a solvent cavity that is one or more shells away from the Na atom. This suggests that there are up to four chemically distinct environments for the electron during the CTTS reaction: the electron resides in the CTTS excited state before detachment and then is ejected either into an immediate contact pair, into a solvent-separated contact pair, or as a free solvated electron. Since each of the four electron environments

(42) The small amplitude of the signals involved, the nonexponential nature of the difference signal dynamics, and the possibility that a fraction of solvent-separated pairs can spontaneously dissociate into free electrons result in extremely large error bars ( $\pm 50\%$ ) in our estimate that the ratio of suppressed to enhanced recombination is unity.

is characterized by different dynamics, we can selectively re-excite the electrons in any one environment by proper choice of the time at which the re-excitation pulse is applied.

If the re-excitation pulse is applied in the first few hundred femtoseconds, before the electron is ejected, the resulting distribution of immediate and solvent-separated contact pairs is similar to that produced if the sum of the pump and re-excitation energies had been supplied in a single photon. This suggests that little dissipation occurs during the excited state lifetime, and that re-excitation during this time serves mainly to increase the spatial extent of the excited-state wave function.

If the re-excitation pulse is applied in the first couple of picoseconds after 780-nm detachment, it acts primarily on electrons in immediate contact pairs. These electrons are undergoing recombination with their geminate partners at a rate of  $\sim 1 \text{ ps}^{-1}$  due to direct overlap of the electrons' wave functions with the sodium atoms in their first solvent shells. The effect of the re-excitation pulse is to promote the localized immediate-pair electron ground state into a highly delocalized excited-state wave function in the fluid's conduction band. This lowers the electron density in the immediate solvent cavity but also increases the degree of contact with the nearby  $\text{Na}^0$ , leading to little net change in the rate of recombination. The excited state of the electron lives for  $\sim 0.5 \text{ ps}$ , decaying by internal conversion back to the ground state, where it again becomes localized in a solvent cavity. The excited state is delocalized enough that roughly one-third of the re-excited electrons do not collapse back into their original cavities; an analysis of how the recombination is suppressed following re-excitation suggests that the majority of these electrons collapse into a solvent cavity one solvent shell away. The fact that both the CTTS detachment and relocalization rates scale the same way in different solvents leads us to believe that similar solvent motions are responsible for both the CTTS detachment and the internal conversion/relocalization of the excited electron. The lifetimes of both the CTTS and solvated electron excited states are limited primarily by the solvent translational motions necessary to form a cavity capable of supporting the solvated electron's ground state.

If the re-excitation pulse is applied more than  $\sim 3 \text{ ps}$  after the original CTTS detachment, it acts primarily on electrons in solvent-separated contact pairs. These electrons have little direct overlap with their geminate partners, which are located one solvent shell away. Thus, they undergo recombination only when a significant fluctuation breaks up the local solvent structure, a process that occurs in THF at room temperature on a hundreds-of-picoseconds time scale. Like the case of electrons in immediate pairs, the effect of the re-excitation pulse is to delocalize the electron's wave function. We expect that this delocalization creates an overlap between the excited solvent-separated electron's wave function and the sodium atom. This overlap allows recombination to take place with a rate similar to that of recombination of the excited immediate-pair electrons, on the order of  $\sim 1 \text{ ps}^{-1}$ . Thus, at early times after re-excitation,

we see an enhancement of recombination: roughly half of the re-excited electrons, which ordinarily would not have recombined for hundreds of picoseconds, undergo recombination in under a picosecond. The delocalized electron excited state then collapses back to the ground state in  $\sim 0.5 \text{ ps}$ , shutting off the enhanced recombination. A significant fraction of these electrons relocalize, ending up as free solvated electrons more than one solvent shell away from the sodium atom. These electrons, which also ordinarily would have recombined in hundreds of picoseconds, now do not recombine at all on subnanosecond time scales, leading to a long-time suppression of the recombination.

Finally, if the re-excitation pulse is applied more than  $\sim 500 \text{ ps}$  after the original CTTS detachment, it acts primarily on free solvated electrons. These electrons have no direct contact with their geminate partners and do not diffusively recombine on subnanosecond time scales. Like each of the previous cases, the effect of the re-excitation pulse is to delocalize the electron's wave function for a period of  $\sim 0.5 \text{ ps}$ . We find that this brief delocalization has essentially no effect on the recombination dynamics. This suggests either that the free electrons are very far away from the sodium atom or that the size of the excited state is small enough that it cannot encompass a sodium atom a few solvent shells away.

The fact that the re-excitation pulse can produce different dynamical processes when applied at different times provides strong evidence that our picture of four distinct environments for the electron is correct. Moreover, the fact that the re-excitation pulse can alter the reaction dynamics allows us a degree of control over how the reaction progresses. This gives us the ability to tailor the distribution of distances between solvated electrons and sodium atoms. Our future goal is to use this ability to study the back ET reaction as the initial distance between the electron and sodium atom is continuously varied: we hope to prepare a desired initial state and then watch the subsequent back ET dynamics.<sup>43</sup> In many ways, this is the experimental analogue to a Monte Carlo or MD calculation of a potential of mean force (although the experimental system of necessity can study only nonequilibrium dynamics). Our hope is that this type of experimental control, combined with the relative simplicity and theoretical tractability of this system, will enable an unprecedented degree of contact between experiment and theory for understanding the dynamics of electron transfer.

**Acknowledgment.** This work was supported by the National Science Foundation under CAREER award CHE-9733218. B.J.S. is an Alfred P. Sloan Foundation Research Fellow, a Cottrell Scholar of Research Corporation, and a Camille Dreyfus Teacher-Scholar.

JA025942D

(43) This idea is similar to that of Closs and Miller (Closs, G.; Miller, J. R. *Science* **1988**, *240*, 440), in which the initial donor/acceptor distance can be finely turned prior to photoinduced charge transfer.